Nanoscale

PAPER

View Article Online
View Journal | View Issue

Cite this: *Nanoscale*, 2022, **14**, 1340

Transient reshaping of intraband transitions by hot electrons†‡

Benjamin T. Diroll *[a] and Tathagata Banerjee [a,b]

Hot electrons, far above the lattice temperature of a material, present opportunities for enhanced solar energy harvesting or performance of otherwise unfavorable chemistry. The spectroscopic signatures and dynamics of hot carrier absorption and emission have been extensively studied in bulk and nanoscopic semiconductors, but the effects on intraband transitions are largely unexplored. Here, the effect of hot electrons on the properties of colloidal quantum wells made of cadmium selenide is examined using ultrafast spectroscopy. Similar to expitaxial quantum wells, these atomically precise materials support intersubband transitions (a class of intraband transitions in 1D and 2D materials) in the near-infrared spectral window. Using energy-dependent photoexcitation, it is shown that electrons reach effective temperatures of 2000 K or greater. This results in a substantial transient shift in the oscillator strength of the intersubband transition to lower energies on a sub-picosecond time-scale. Similar heating of electrons is achieved under mid-infrared re-excitation, which permits ultrafast transmittance modulation throughout the near-infrared.

Received 21st September 2021,
Accepted 31st December 2021

DOI: 10.1039/d1nr06203d

rsc.li/nanoscale

[a]*Center for Nanoscale Materials, Argonne National Laboratory, USA. E-mail: bdiroll@anl.gov*

[b]*Department of Physics, University of Illinois Urbana-Champaign, USA*

† Electronic supplementary information (ESI) available: Materials, synthesis, and methods details as well as additional data. See DOI: 10.1039/d1nr06203d

Benjamin T. Diroll

Benjamin T. Diroll received his PhD in chemistry from the University of Pennsylvania (2015). Subsequently, he become a Director's postdoctoral fellow and then a scientific staff member at the Center for Nanoscale Materials at Argonne National Laboratory. His research interests include synthesis, self-assembly, optical properties, and device physics of nanomaterials.

Introduction

Hot carriers, which may have non-thermal energy distributions or effective temperatures above that of the material lattice, are important for many optoelectronic devices.[1] They have been used in Gunn diodes for 60 years and more recent work has focused on the enhancing photovoltaic efficiency by exploiting the extra potential energy above the band gap[2,3] or in photochemical reactions, where hot carriers lift contraints of band edge energies.[4–6] The primary tool for studying hot carriers, due to their short lifetime, is time-resolved spectroscopy: many works have demonstrated the transient changes in band gap absorption or emission arising from hot carriers in semiconductors and metals.[7–11] Yet there are few demonstrations of hot carrier effects on intraband transitions.[12–14]

This work studies the effects of hot electrons on intraband transitions using cadmium selenide colloidal quantum wells (CQWs), which exhibit a class of intraband transitions, termed intersubband transitions, from the first to second conduction bands occuring in the near-infrared. Because intersubband transitions are the critical element of quantum cascade lasers[15] and quantum well infrared photodetectors,[16] the effects of hot electrons on these intraband transitions can alter gain spectra, thresholds, or current levels.[17]

Using variable pump energy ultrafast pump–probe spectroscopy, we find the dominant spectroscopic signature of hot electrons in CdSe CQWs is a sub-picosecond broadening and redshift of the intersubband transition, which is quantitatively approximated with a Boltzman distribution for electron temp-

erature. With pump energies in excess of the band gap, hot electrons in the CQWs may reach effective temperatures higher than 2000 K, before cooling back to ambient temperature in less than 1 ps. Additionally, it is shown that photoexcitation of electrons already in the conduction band generates a similar spectral response to high energy photoexcitation, yielding sub-picosecond modulation at near-infrared wavelengths.

Results and discussion

Cadmium selenide CQWs are sheets consisting, in this case, of 4, 5, or 6 layers of cadmium selenide with an additional capping layer of cadmium atoms, to form 4.5, 5.5, or 6.5 monolayer (ML) structures. The electronic structure of the CQWs is shown alongside the absorption of the samples in Fig. 1. Quantum confinement in the thin axis of the CQWs results in a steplike density of states by allowed transitions between the main levels of electrons and holes, with holes further are split into heavy-hole (HH), light-hole (LH), and split-off (SO) bands.[18] Atop the continuous transitions are the strong excitonic absorptions which dominate at room temperature due to the large exciton binding energy (>150 meV) of the samples.

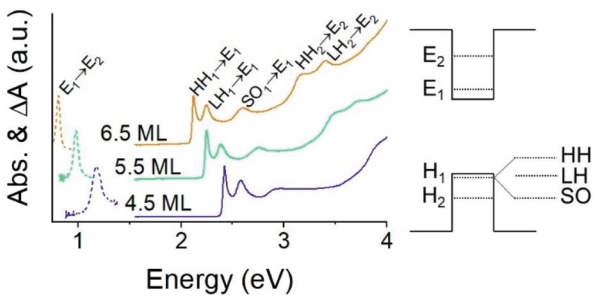

Fig. 1 Normalized absorption (solid lines) and photoinduced absorption (dashed lines) of the CdSe CQW samples used in this work. Spectroscopically observed transitions are labelled conventionally according to the energy diagram at right.

When photoexcited or doped, CQWs also show well-defined intraband transitions, shown with dashed lines in Fig. 1, between the first (E_1) and second (E_2) electron levels.[19] Because the E_1 and E_2 levels of a quantum well are bands, not discreet states, these intraband optical transitions are often called intersubband transitions.[20]

Despite their use in optoelectronic devices such as quantum well infrared photodetectors and quantum cascade lasers, intersubband transitions have not been extensively studied spectroscopically for their non-equilibrium electronic behaviour. Limited earlier reports indicate the substantial spectral reshaping of mid-infrared intersubband transitions in GaAs epitaxial quantum wells.[12,13] Here, the influence of hot electrons in the optical properties of intersubband transitions are examined by transient absorption spectroscopy with variable pump photon energy excitation. Fig. 2 shows the transient absorption data over the first picosecond of pump–probe delay for 4.5, 5.5, and 6.5 ML cadmium selenide CQWs. The upper pseudocolor plots show the transient response under resonant excitation of the lowest excitonic absorption of the sample. The lower plots show the samples excited with photons approximately 0.85 eV greater than the band gap energy. In all cases, the fluence of the pump generates an average of less than 0.3 excitons per particle.

More energetic pump excitation results in a transient tail of absorption at lower energy than the transitions in Fig. 1. This shift is obscured in the 6.5 ML sample due to the detector cut-off at 0.76 eV. Nonetheless, the data in Fig. 2 provide a strong indication that the dominant effect of high effective electron temperature (T_e) is a red-shift and broadening of the intersubband transitions. This contrasts with the previous examples of hot electron studies on quantum wells showing a small blue-shift and broadening of the intersubband transition.[12,13] Additionally, the timescale of transient spectral changes increases with the thickness of the CQW: Fig. S4 and Table S1† show that more energetic excitation results in slower filling of the conduction band minimum (despite similar excess energy from the absorbed photons), with the rise times increasing from 4.5 ML (188 ± 56 fs) to 6.5 ML (464 ± 142 fs).

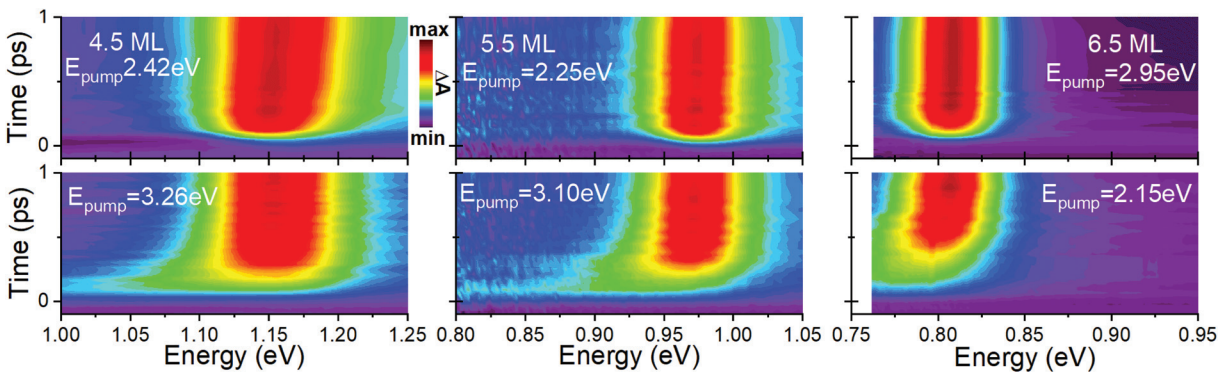

Fig. 2 Near-infrared transient absorption data for (top) 4.5 ML, 5.5 ML, and 6.5 ML CdSe CQW samples with resonant excitation of the lowest excitonic absorption. (bottom) The same samples with pump photon energy above the band gap. The fluence was maintained to generate an average of less than 0.3 excitons per particle.

A quantitative evaluation of the role of hot electrons in the transient reshaping of the intersubband transitions requires consideration of several potential changes induced by elevated T_e. Related optical responses of semiconductor materials at the band gap due to hot electrons are well understood through transient photoluminescence and absorption or reflectance measurements.[7–11,21] At least three effects may be observed on the spectral response which are considered in this case: Moss–Burstein shifts;[21–23] band gap renormalization;[12] and transition line-width and energy changes due to changed electron distribution in bands.[7,10,11,24] The cartoons in Fig. 3a provide pictures of these processes.

For the data presented in Fig. 2, Moss–Burstein shifts of the band gap (or intraband transitions) are not anticipated because the number of photogenerated excitons is low, averaging less than 1 exciton per CQW or electron sheet densities of 2–5 × 10^{11} cm^{-2}.[25–30] Because the radiative lifetime is also much longer (nanoseconds) than intraband relaxation, the results in the first picosecond of pump–probe delay are not expected to reflect changes in carrier density. (At higher initial densities and longer delay times, Burstein–Moss effects are likely responsible for a 25 meV blueshift intersubband absorption which occurs concomitant with recombination as shown in Fig. S5†). Similar conclusions may be reached regarding band gap renormalization (BGR). BGR is also fluence-dependent[31] and consists chiefly of a reduction in the absolute energy of the E_1 band. Reported band gap renormalization for E_1 is less than 20 meV in III–V quantum wells at excitation intensities like those used here. The effects of renormalization on the unfilled E_2 band are a factor of ten smaller,[32–34] meaning, on net, BGR may produce a blue-shift of the intersubband transition of 20 meV or less.[33,35] Effects of BGR related to carrier distribution—*i.e.* T_e—are even smaller (<10 meV).[36]

Spectroscopic evidence indicates that band gap renormalization is not a substantial effect here because the observed shift from hot electrons is asymmetric, much larger in scale, and the opposite direction (in energy) from band gap renormalization. Additionally, because renormalization reflects the occupation of the lowest conduction band, this effect should also persist on a time-scale of recombination (*i.e.* nanoseconds), rather than femtoseconds.[37] Indeed, as noted above, spectral shifts at higher excitation intensities are opposite the expectations of BGR and more in line with Moss–Burstein effects. Neither Moss–Burstein or BGR appears significantly in the low fluences and early times analysed in Fig. 2.

The dominant effect of hot electrons in the intersubband transitions of cadmium selenide CQWs is the presence of low-energy absorption, as is shown in the shaded region of Fig. 3b. It is straightforward to understand how the transition changes at higher T_e: greater occupation of the E_1 band (Fig. 3a, upper cartoon) reduces the energy difference with E_2. The transitions available are determined by differences in the dispersion of the first and second conduction bands.[38,39] Here, using the effective mass models which predict the quasi-particle gap of CQWs,[18,40] the electron effective mass of the E_1 band may be estimated as 0.13; effective masses for E_2 band of the 4.5, 5.5, and 6.5 ML samples are estimated at 0.25, 0.22, and 0.21, respectively (see Fig. S1†).

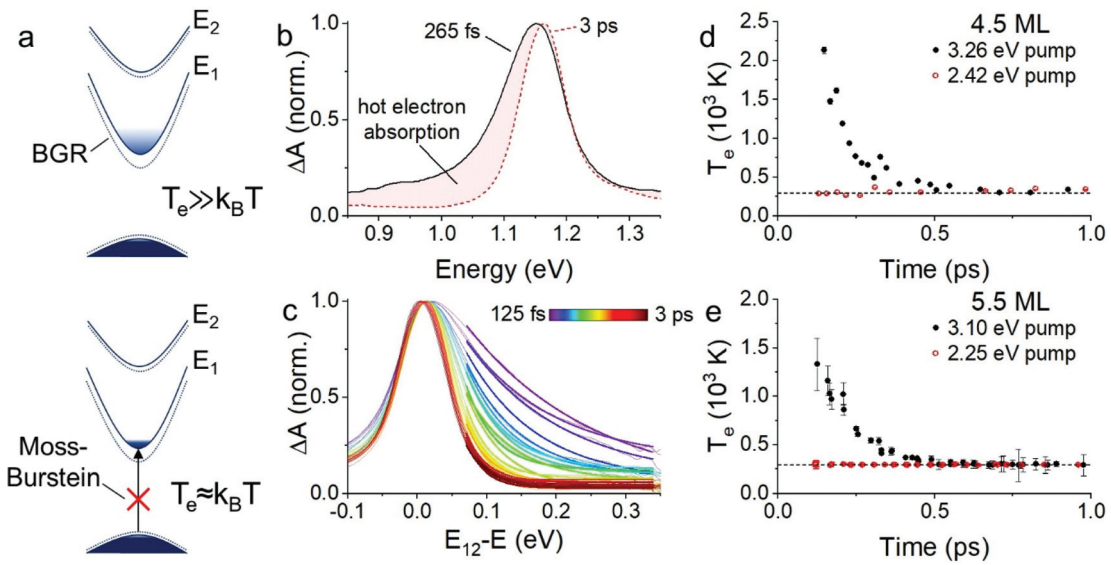

Fig. 3 (a) Cartoons of intersubband and interband transitions under conditions of high electron temperature (top) and quasi-equilibrium electron temperature (bottom). BGR stands for band gap renormalization. (b) Spectral line-cuts of transient absorption spectrum of 4.5 ML CQWs photo-excited with 3.26 eV pump photons. (c) Spectral line-cuts of the same sample as a function of time with a normalized energy coordinate ($E_{12} - E$). Thin lines indicate experimental data; thick lines show the region fitted with a Boltzman distribution. (d and e) Fitted values of T_e for (d) 4.5 ML and (e) 5.5 ML CQW samples under the different pump excitation conditions specified in the caption. The dashed lines in (d) and (e) indicate the ambient temperature of the measurement.

A large body of literature on the effect of hot carriers on the band transitions of semiconductors shows that optical response can be effectively modelled using the equilibrium extinction and T_e.[7,10,11,24] In semiconductors—including CQWs—hot carriers result in photoluminescence or transient bleaching at energies above the band gap, which may be modelled with a Boltzmann distribution.[10,41–43] Applying this methodology to the transient reshaping of intersubband transitions requires normalizing the energy coordinate relative to the equilibrium transition energy (here labelled E_{12}) since the observed photoinduced absorption feature is at lower, rather than higher, energy. This inversion of the energy scale is due to a joint optical density of states which increases at energies below E_{12}, opposite the case of interband transitions above a band gap, as shown in the ESI†. No further scaling of the energy scale to account for band dispersions has been performed here, as previous works developed this methodology without k selection rules on transitions.[9–11,44,45] Similarly, fixed k transitions cannot explain observed non-inversion optical gain in quantum cascade lasers or tail absorption; such results in epitaxial wells require phonon-coupled transitions[46–50] (see ESI† for extended discussion). Reframed in this manner, as in Fig. 3c, the thermally excited population of electrons is manifest as a tail to higher energy relative to the transition energy, just as in previous studies at the band gap. This tail may be fitted to a Boltzmann distribution:

$$\Delta A(E_{12}-E) = \Delta A_0(E_{12}-E)e^{\frac{E_{12}-E}{k_B T_e}}.$$

Importantly, the establishment of a carrier distribution which may be described by T_e is not instantaneous. For excitation above the band gap, an initially non-thermal distribution evidenced in Fig. S6† adopts a thermal distribution after c. 120 fs due to electron–electron scattering. Fitting results for the 4.5 ML and 5.5 ML samples are shown in Fig. 3d and e, respectively. Too little data below the energy of the intersubband transition of the 6.5 ML sample was obtained to estimate carrier temperature using this methodology (a similar fact is also the reason for larger error estimates for the 5.5 ML sample). As show in Fig. 3, T_e with excitation above the band gap reaches as high as 2000 K before falling back to the ambient temperature within 500 fs. This result is broadly consistent with measurements on ultrafast cooling of core/shell CQWs using two-photon photoemission spectroscopy.[51] That work showed electron temperatures reaching 3000 K (with greater excess pump energy than in this work) and returning to room temperature in less than 1 ps. As shown in the ESI,† the estimated temperatures are lower than those predicted based upon an estimate of the electronic heat capacity of the CQWs, using literature data on CdSe quantum dots.[52] At least part of this discrepancy may arise form the pump–probe delay before which an estimate of carrier temperature is obtained.

Like the dynamics line cuts at the intersubband peak energy (Fig. S4†), the evolution of T_e also indicates faster cooling in thinner CQWs. If LO phonons are the primary cooling pathway, as typically observed, this can be quantified by estimating the time constant (τ_0) of LO phonon relaxation based upon the energy loss of the system:[11,42,53]

$$\frac{dE}{dT} = \frac{3k_B}{2}\frac{dT_e}{dt} \approx \frac{E_{LO}}{\tau_0}\left(e^{-\frac{E_{LO}}{k_B T_e}} - e^{-\frac{E_{LO}}{k_B T_L}}\right)$$

In which E_{LO} is the energy of LO phonons (25.4 meV in both thicknesses of platelet[54]), and T_L is the lattice temperature (fixed at 292 K). Energy loss data for the samples are shown in Fig. S7.† Values of τ_0 for the first picosecond of data are 13 ± 8 fs and 20 ± 8 for 4.5 ML and 5.5 ML, respectively. These values somewhat faster than the 33 fs estimate for even thicker core/shell CQWs.[51] An additional possibility for the faster cooling of thinner CQWs is that surface phonon modes (not just LO phonons) play an important role in cooling, which was also suggested previously.[55,56]

The line-shape of the intersubband transition also reveals fluence-dependence of the dynamics. The cooling times observed here under low fluence excitation are much faster than those reported at higher fluence.[43] T_e *versus* pump–probe delay is shown for several pump intensities in Fig. 4 (log-linear scale data are in Fig. S8†). At fluences which generate less than one electron–hole pair per CQW the density of the excitation is the same on a per particle basis and T_e decays in a power-independent manner to ambient temperature in less than 1 ps, similar to two-photon photoemission experiments.[51] At a fluence which generated 3.5 electron–hole pairs per CQW, T_e reaches a somewhat higher peak and electron cooling occurs in two stages: rapid cooling on a sub-picosecond time-scale followed by a prolonged, slower decay of T_e. This second, slower decay, may be interpreted as a substantial elongation of τ_0, termed a hot phonon bottleneck. However, Auger recombination also offers an explanation for prolonged T_e elevation.[57] Such exciton–exciton interactions can be suppressed by localization of excitons at spatially distinct areas on the CQW, which may be responsible for the higher density onset of slowed T_e decay, which are not observed for an average exciton density of 1.1.[58,59]

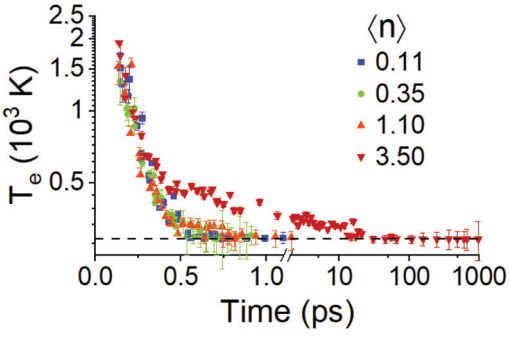

Fig. 4 Electron temperature *versus* time for a 5.5 ML CQW sample excited at 3.10 eV. The figure label indicates the average number of electron–hole pairs generated and the dashed line indicates the ambient temperature.

In addition to the generation of hot electrons through interband excitation above the band gap energy, intraband excitation of electrons in the conduction band also produces elevated T_e. Because the CQWs are undoped as synthesized, this is achieved here using multiple photoexcitations in a pump–push–probe experiment. An initial (chopped) pump pulse at 3.10 eV was used to excite an ensemble of 5.5 ML CQWs. Initial cooling of the photoexcited carriers was allowed for 15 ps before a subsequent push pulse in the mid-infrared (0.41 eV) excited the electrons in the conduction band of the CQWs. The mid-infrared pulse couples into a weak, continuous photoinduced absorption in the infrared, as the precise wavelength of choice centered between 0.46 eV and 0.20 eV did not change the spectroscopic observables. At the same time, however, the mid-infrared pulse was well below the energy of the intersubband transition itself (0.96 eV). The result is that the push excitation heats electrons within the E_1 band, but does not promote them to the E_2 band, analogous to heating of carrier plasmas in doped semiconductors or metals.

As shown in Fig. 5a, the infrared pulse sharply reduces the peak intensity of the intersubband absorption feature. Like the transient signals with interband excitation, the intersubband absorption transiently broadens and redshifts. Before recovering within 1 ps after the push pulse. Using the same methodology to that applied to the transient response after interband excitation, T_e is extracted from the spectral transients. The effective electron temperature peak after push excitation at approximately 1000 K. This peak is lower than observed under interband excitation, but the photon energy in this case is only 0.41 eV. Electron heating and excess pump energy is not a simple proportionality due to the temperature-dependence of electron heat capacity. As with the rapid decay of T_e shown in Fig. 3, the rise and fall of T_e with the push excitation also occurs in less than 1 picosecond.

The non-resonant modulation of near-infrared transmission is common to all thicknesses. By changing temperature or sample thickness, the energies (wavelengths) of light which may be modulated using push pulses can be selected as well as the type of change (increased/decreased absorption). These include common telecommunications wavelengths. Fig. S9† shows absorption modulation at 1.3 μm and 1.55 μm for the various samples, with a peak absorption modulation at 1.55 μm reaching 60% in the case of 6.5 ML samples. Compared to previous examples in epitaxial quantum wells,[60] these results encompass a larger energy range, higher absolute energies (shorter wavelengths), and narrower band width for optical modulation.

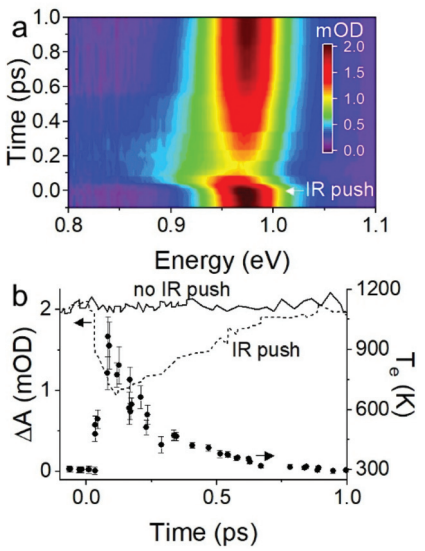

Fig. 5 (a) Map of transient absorption of 5.5 ML CQW sample with a 3.10 eV pump excitation followed by a 0.35 eV push excitation of the photoexcited carriers. The time axis is defined with respect to the push–probe delay. (b) Temporal line-cuts of near-infrared absorption with (dashed line) a push pulse and without a push pulse (solid line). Data points show the electron temperature as a function of push–probe delay.

Conclusions

Hot electrons drive transient reshaping of intersubband transitions in CQWs. This effect, which is dominated by a broadening and redshift of the transitions on a sub-picosecond timescale, is only apparent when electrons are excited with additional energy above the conduction band minimum. A modified fitting procedure is adapted from analysis of the band absorption to yield a quantitative estimate of electron temperature. The transient broadening of the intraband transition in CQWs reveals electron temperatures as high as 2000 K. Under low fluence excitation, the electron temperature falls close to room temperature in less than 1 ps, but under conditions generating multiple electron–hole pairs per CQW, cooling can be prolonged by a factor of 100. Finally, multiple pump excitation is used to thermally excite electrons in the CQW conduction band, which permits the sub-picosecond modulation of near-infrared light transmission at telecommunications wavelengths.

Conflicts of interest

There are no conflicts to declare.

Acknowledgements

Use of the Center for Nanoscale Materials and Advanced Photon Source, both Office of Science user facilities, was supported by the U.S. Department of Energy, Office of Science, Office of Basic Energy Sciences, under Contract no. DE-AC02-06CH11357. This work was supported in part by the U.S. Department of Energy, Office of Science, Office of Workforce Development for Teachers and Scientists (WDTS) under the Science Undergraduate Laboratory Internships Program (SULI).

Notes and references

1 S. Luryi, in *Hot Electrons in Semiconductors: Physics and Devices*, ed. N. Balkan, Claredon Press, Oxford, 1998, pp. 385–427.
2 R. T. Ross and A. J. Nozik, *J. Appl. Phys.*, 1982, **53**, 3813–3818.
3 D. Knig, K. Casalenuovo, Y. Takeda, G. Conibeer, J. F. Guillemoles, R. Patterson, L. M. Huang and M. A. Green, *Phys. E*, 2010, **42**, 2862–2866.
4 S. Mukherjee, F. Libisch, N. Large, O. Neumann, L. V. Brown, J. Cheng, J. B. Lassiter, E. A. Carter, P. Nordlander and N. J. Halas, *Nano Lett.*, 2013, **13**, 240–247.
5 Y. Zhang, S. He, W. Guo, Y. Hu, J. Huang, J. R. Mulcahy and W. D. Wei, *Chem. Rev.*, 2018, **118**, 2927–2954.
6 L. Zhou, D. F. Swearer, C. Zhang, H. Robatjazi, H. Zhao, L. Henderson, L. Dong, P. Christopher, E. A. Carter, P. Nordlander and N. J. Halas, *Science*, 2018, **362**, 69–72.
7 G. Lasher and F. Stern, *Phys. Rev.*, 1964, **133**, A553–A563.
8 J. Shah, C. Lin, R. F. Leheny and A. E. DiGiovanni, *Solid State Commun.*, 1976, **18**, 487–489.
9 C. V. Shank, R. L. Fork, R. F. Leheny and J. Shah, *Phys. Rev. Lett.*, 1979, **42**, 112–115.
10 R. F. Leheny, J. Shah, R. L. Fork, C. V. Shank and A. Migus, *Solid State Commun.*, 1979, **31**, 809–813.
11 D. Von Der Linde and R. Lambrich, *Phys. Rev. Lett.*, 1979, **42**, 1090–1093.
12 R. J. Bäuerle, T. Elsaesser, H. Lobentanzer, W. Stolz and K. Ploog, *Phys. Rev. B*, 1989, **40**, 10002–10005.
13 T. Elsaesser, R. J. Bäuerle and W. Kaiser, *Solid-State Electron.*, 1989, **32**, 1701–1705.
14 G. B. Serapiglia, K. L. Vodopyanov and C. C. Phillips, *Appl. Phys. Lett.*, 2000, **77**, 857–859.
15 J. Faist, F. Capasso, D. Sivco, C. Sirtori, A. L. Hutchinson and A. Y. Cho, *Science*, 1994, **264**, 553–556.
16 B. F. Levine, *J. Appl. Phys.*, 1993, **74**, R1–R81.
17 B. Etienne, J. Shah, R. F. Leheny and R. E. Nahory, *Appl. Phys. Lett.*, 1982, **41**, 1018–1020.
18 S. Ithurria, M. D. Tessier, B. Mahler, R. P. S. M. Lobo, B. Dubertret and A. L. Efros, *Nat. Mater.*, 2011, **10**, 936–941.
19 B. T. Diroll, M. Chen, I. Coropceanu, K. R. Williams, D. V. Talapin, P. Guyot-Sionnest and R. D. Schaller, *Nat. Commun.*, 2019, **10**, 4511.
20 M. Helm, in *Intersubband Transitions in Quantum Wells: Physics and Device Applications I*, ed. F. Capasso, Academic Press, New York, 1999, pp. 1–99.
21 J. Shah, R. F. Leheny and C. Lin, *Solid State Commun.*, 1976, **18**, 1035–1037.
22 T. S. Moss, *Proc. Phys. Soc., London, Sect. B*, 1954, **67**, 775–782.
23 E. Burstein, *Phys. Rev.*, 1954, **93**, 632–633.
24 S. Tanaka, H. Kobayashi, H. Saito and S. Shionoya, *J. Phys. Soc. Jpn.*, 1980, **49**, 1051–1059.
25 C. Delalande, G. Bastard, J. Orgonasi, J. A. Brum, H. W. Liu, M. Voos, G. Weimann and W. Schlapp, *Phys. Rev. Lett.*, 1987, **59**, 2690–2692.
26 G. Tränkle, H. Leier, A. Forchel, H. Haug, C. Ell and G. Weimann, *Phys. Rev. Lett.*, 1987, **58**, 419–422.
27 U. Bockelmann, P. Hiergeist, G. Abstreiter, G. Weimann and W. Schlapp, *Surf. Sci.*, 1990, **229**, 398–401.
28 Y. H. Zhang, R. Cingolani and K. Ploog, *Phys. Rev. B*, 1991, **44**, 5958–5961.
29 S. Haacke, R. Zimmermann, D. Bimberg, D. E. Mars and J. N. Miller, *Superlattices Microstruct.*, 1991, **9**, 27–30.
30 D. A. Kleinman and R. C. Miller, *Phys. Rev. B*, 1985, **32**, 2266–2272.
31 H. Haug and S. W. Koch, *Phys. Rev. A*, 1989, **39**, 1887–1898.
32 I. Abram and J. A. Levenson, *Superlattices Microstruct.*, 1989, **5**, 181–184.
33 J. C. Ryan and T. L. Reinecke, *Phys. Rev. B*, 1993, **47**, 9615–9620.
34 J. A. Levenson, I. Abram, R. Raj, G. Dolique, J. L. Oudar and F. Alexandre, *Phys. Rev. B*, 1988, **38**, 13443–13446.
35 V. D. Kulakovskii, E. Lach, A. Forchel and D. Gïtzmacher, *Phys. Rev. B*, 1989, **40**, 8087–8090.
36 H. Wang, J. Shah, T. C. Damen, S. W. Pierson, T. L. Reinecke, L. N. Pfeiffer and K. West, *Phys. Rev. B*, 1995, **52**, R17013–R17016.
37 R. Cingolani, H. Kalt and K. Ploog, *Phys. Rev. B*, 1990, **42**, 7655–7658.
38 P. von Allmen, M. Berz, G. Petrocelli, F.-K. Reinhart and G. Harbeke, *Semicond. Sci. Technol.*, 1988, **3**, 1211–1216.
39 M. Załużny, *Phys. Rev. B*, 1991, **43**, 4511–4514.
40 A. R. Greenwood, S. Mazzotti, D. J. Norris and G. Galli, *J. Phys. Chem. C*, 2021, **125**(8), 4820–4827.
41 D. Zanato, N. Balkan, B. K. Ridley, G. Hill and W. J. Schaff, *Semicond. Sci. Technol.*, 2004, **19**, 1024–1028.
42 K. Kash and J. Shah, *Appl. Phys. Lett.*, 1984, **45**, 401–403.
43 M. Pelton, S. Ithurria, R. D. Schaller, D. S. Dolzhnikov and D. V. Talapin, *Nano Lett.*, 2012, **12**, 6158–6163.
44 G. Göbel, *Appl. Phys. Lett.*, 1974, **24**, 492–494.
45 R. F. Leheny and J. Shah, *Phys. Rev. Lett.*, 1977, **38**, 511–514.
46 R. Terazzi, T. Gresch, M. Giovannini, N. Hoyler, N. Sekine and J. Faist, *Nat. Phys.*, 2007, **3**, 329–333.
47 H. Willenberg, G. H. Döhler and J. Faist, *Phys. Rev. B*, 2003, **67**, 1–10.
48 C. Ndebeka-Bandou, F. Carosella, R. Ferreira, A. Wacker and G. Bastard, *Appl. Phys. Lett.*, 2012, **101**, 191104.
49 C. Ndebeka-Bandou, F. Carosella, R. Ferreira and G. Bastard, *Appl. Phys. Lett.*, 2013, **102**, 191105.
50 F. Carosella, C. Ndebeka-Bandou, R. Ferreira, E. Dupont, K. Unterrainer, G. Strasser, A. Wacker and G. Bastard, *Phys. Rev. B*, 2012, **85**, 085310.
51 P. Sippel, W. Albrecht, J. C. Van Der Bok, R. J. A. Van Dijk-Moes, T. Hannappel, R. Eichberger and D. Vanmaekelbergh, *Nano Lett.*, 2015, **15**, 2409–2416.
52 S. Neeleshwar, C. C. L. Chen, C. B. Tsai, Y. Y. Chen, C. C. L. Chen, S. G. Shyu and M. S. Seehra, *Phys. Rev. B*, 2005, **71**, 6–9.
53 Y. Yang, D. P. Ostrowski, R. M. France, K. Zhu, J. van de Lagemaat, J. M. Luther and M. C. Beard, *Nat. Photonics*, 2015, **10**, 53–59.

54 B. T. Diroll, W. Cho, I. Coropceanu, S. M. Harvey, A. Brumberg, N. Holtgrewe, S. A. Crooker, M. R. Wasielewski, V. B. Prakapenka, D. V. Talapin and R. D. Schaller, *Nano Lett.*, 2018, **18**, 6948–6953.
55 B. T. Diroll and R. D. Schaller, *ACS Nano*, 2020, **14**, 12082–12090.
56 D. Bozyigit, N. Yazdani, M. Yarema, O. Yarema, W. M. M. Lin, S. Volk, K. Vuttivorakulchai, M. Luisier, F. Juranyi and V. Wood, *Nature*, 2016, **531**, 618–622.
57 M. Achermann, A. P. Bartko, J. A. Hollingsworth and V. I. Klimov, *Nat. Phys.*, 2006, **2**, 557–561.
58 Q. Li, Q. Liu, R. D. Schaller and T. Lian, *J. Phys. Chem. Lett.*, 2019, **10**, 1624–1632.
59 P. Geiregat, C. Rodá, I. Tanghe, S. Singh, A. Di Giacomo, D. Lebrun, G. Grimaldi, J. Maes, D. Van Thourhout, I. Moreels, A. J. Houtepen and Z. Hens, *Light: Sci. Appl.*, 2021, **10**, 112.
60 J. D. Heber, C. Gmachl, H. M. Ng and A. Y. Cho, *Appl. Phys. Lett.*, 2002, **81**, 1237–1239.